Short title

BNP is required for male gametogenesis

Title

The DC1 domain protein BINUCLEATE POLLEN is required for pollen development in Arabidopsis

Author's names and affiliations

Leonardo Agustín Arias[1], Sebastián D'Ippolito[1], Jésica Frik[1], Natalia Loreley Amigo, Claudia Anahí Casalongué, Gabriela Carolina Pagnussat, Diego Fernando Fiol[2]

Instituto de investigaciones Biológicas IIB-CONICET- Universidad Nacional de Mar del Plata, Mar del Plata, Buenos Aires, 7600, Argentina.

Footnotes

Author contributions

D.F.F. conceived the original screening and research plans; D.F.F., G.C.P. and C.A.C. supervised the experiments; L.A.A., S.D., J.F. and N.L.A. performed most of the experiments; D.F.F., G.C.P and L.A.A. designed the experiments and analyzed the data; D.F.F. conceived the project and wrote the article with contributions of all the authors; D.F.F. agrees to serve as the author responsible for contact and ensures communication.

[1] these authors contributed equally to this work.

[2] Author for contact: Diego Fernando Fiol (diefiol@mdp.edu.ar) Tel +54 2234753030

One sentence summary

The DC1 domain protein BNP is required for pollen development and germination by mediating NAC transcription factors VOZ1/2 nuclear localization.

Abstract

Development of the male gametophyte is a tightly regulated process that requires precise control of cell division and gene expression. A relevant aspect to understand the events underlying pollen development regulation constitutes the identification and characterization of the genes required for this process. In this work we showed that the DC1 domain protein BINUCLEATE POLLEN (BNP) is essential for pollen development and germination. Pollen grains carrying the defective *BNP* allele failed to complete mitosis II and are impaired in pollen germination. By yeast two hybrid screening and bimolecular fluorescence complementation assays, we identified a set of BNP-interacting proteins. Among confirmed interactors we found NAC family transcriptional regulators Vascular plant One-Zinc finger 1 (VOZ1) and VOZ2. BNP and VOZ1/2 proteins were mainly detected co-localized in prevacuolar compartments. As *voz1voz2* double mutants showed the same developmental defect observed in *bnp* pollen grains, we propose that BNP requirement to complete microgametogenesis could be linked to its interaction with VOZ1/2 proteins. By studying VOZ1 localization in pollen from *bnp/BNP* plants, we showed that VOZ1 nuclear localization requires BNP. We propose that BNP is acting as a scaffold protein recruiting VOZ1 and likely VOZ2 to prevacuolar compartments into assemblies that could modulate VOZ1/2 translocation to the nucleus and therefore modulate their activity as transcriptional regulators.

INTRODUCTION

The development of the male gametophyte of flowering plants (pollen grain) takes place inside the anthers and involves two sequential phases: microsporogenesis and microgametogenesis. Microsporogenesis begins when a diploid microsporocyte undergoes meiotic division to form a tetrad of haploid microspores (Twell, 2011). During microgametogenesis a large vacuole is formed inside the released microspores and positions the nucleus in the periphery of the cell. This stage is followed by an asymmetric division or Pollen Mitosis I (PMI) that yields a large vegetative cell and a small germ cell. The germ cell is subsequently engulfed within the cytoplasm of the vegetative cell.

The germ cell then undergoes a second division, Pollen Mitosis II (PMII), which results in twin sperm cells and yields the mature tricellular pollen. In species such as *Arabidopsis thaliana*, PMII takes place inside the pollen grain prior to anthesis. Although transcriptional studies have provide significant advances in the understanding of the molecular mechanisms controlling male gametophyte development, the picture is still far from complete (reviewed in (Hafidh et al., 2016). Studies on isolated mutants have also proved to be of great importance to identify novel genes and cellular mechanisms involved in this process (Borg et al., 2009).

Divergent C1 (DC1) domains are cysteine/histidine-rich zinc finger modules found exclusively in the plant Kingdom. DC1 domains resemble the C1 domains present in PKC and in over a dozen of animal proteins (Colon-Gonzalez and Kazanietz, 2006). However, C1 domains are not frequent in plants, as they were only identified in diacylglycerol kinases (Escobar-Sepúlveda et al., 2017). C1 domains have the ability to bind the secondary messenger diacylglycerol (DAG) but also participate in protein-protein interactions and in the targeting of proteins to the membrane (Colon-Gonzalez and Kazanietz, 2006). Sequence and structure similarities between DC1 and C1 domains suggest that some of the roles played by C1 domains in animal proteins could be fulfilled in plants by DC1 domains (D'Ippólito et al., 2017).

The Arabidopsis genome encodes for over 140 uncharacterized proteins harboring DC1 domains. Reports regarding genes coding for DC1 domain proteins were limited to transcriptional responses. In Arabidopsis, *At5g17960* was described as responsive to hormones and stress treatments (Bhaskar et al., 2015) and *ULI3 (At5g59920)* was related to UV-B responses (Suesslin and Frohnmeyer, 2003). In other plant species, DC1 domain proteins have been also associated with stress and hormone responses (Shinya et al., 2007; Li et al., 2010; Hwang et al., 2014; Gao et al., 2016).

The first functional characterization of a DC1 domain protein, Vacuoleless Gametophytes (VLG), was recently reported (D'Ippólito et al., 2017). VLG localizes to prevacuolar compartments and it was proved to be essential for the development of the female and male gametophytes. A role for VLG was proposed during vacuole biogenesis, likely through the interaction with

the VAMP protein PVA12 and the GDSL-motif lipase LTL1 (D'Ippólito et al., 2017).

In this work we identified the DC1 domain protein BINUCLEATE POLLEN (BNP) as an essential protein for male gametophyte development in Arabidopsis. In addition, we demonstrated that BNP is required for pollen germination and early sporophytic developmental stages. To functionally characterize BNP we searched for protein interactors and identified transcriptional regulators VOZ1 and VOZ2 as BNP binding proteins. Furthermore, we showed that VOZ proteins co-localize to BNP, supporting a physiological interaction. As *voz1voz2* mutants also exhibit pollen developmental defects (Celesnik et al., 2013), we propose that the interaction between BNP and VOZ proteins outside the nucleus might impact on VOZ1/2 activities, resulting in functional consequences for gene expression. By studying VOZ1 localization in a *bnp* mutant background, we showed that VOZ1 nuclear localization requires BNP. Thus, BNP could act as a scaffold protein recruiting VOZ1/2 and likely other proteins to prevacuolar compartments into assemblies that might modulate VOZ1/2 translocation to the nucleus and therefore their activity as transcriptional regulators.

RESULTS

BNP codes for a DC1 domain containing protein

At2g44370, here named *BINUCLEATE POLLEN* (*BNP*), is a single exon gene that encodes for a 250-amino acid long protein with three DC1 domains (Fig. 1B). Phylogenetic analysis of Arabidopsis DC1 domain protein family grouped BNP into the most divergent cluster, being VLG its closest homolog (Fig. 1C). Multiple sequence alignments of selected protein sequences of this cluster and DC1 domain proteins from *C. annuum*, tobacco, wheat and cotton showed amino acid conservation mostly restricted to the residues that define the DC1 signature motif, which might be involved in Zn^2 coordination and folding of the domain (Fig. 1D). On the other hand, amino acids corresponding to loop regions in the folded domain -which might define its binding capabilities (Rahman and Das, 2015)- showed very low similarity, suggesting a diversity of interactors for the aligned proteins.

bnp is a gametophytic mutation

Two Arabidopsis lines with T-DNA insertions in *BNP* (SALK_114889 –here named *bnp-1* and GK-008E01 -here named *bnp-2*) were studied (Fig. 1A). After backcrossing to the Col-0 ecotype, the progeny of self-crossed plants was genotyped. No homozygous mutant plants were recovered in the offspring from *bnp-1/BNP* or *bnp-2/BNP* self-pollinated plants. The ratio of hemizygous to WT plants in the progeny of self-fertilized *bnp-1/BNP* plants was 1.44 (n = 183). For *bnp-2/BNP* plants, segregation analysis for sulfadiazine resistance showed a ratio of resistant to sensitive plants of 1.31 (n = 2634). The proportion of plants harboring the transgene recovered in the progeny of self-fertilized plants was lower than the Mendelian segregation ratio expected for diploid sporophytic (3:1) or embryo lethal (2:1) mutants suggesting a gametophytic defect. Furthermore, no obvious sporophytic phenotypes were observed in the hemizygous plants, suggesting that *bnp* is a recessive mutation (Fig. S1). The siliques of *bnp/BNP* plants showed a small percentage of aborted seeds, not different to WT plants (Fig. S1).

As no homozygous plants were recovered and siliques from hemizygous plants looked normal, the *BNP* mutation could be affecting pollen development or germination. To test this hypothesis, we performed reciprocal crosses

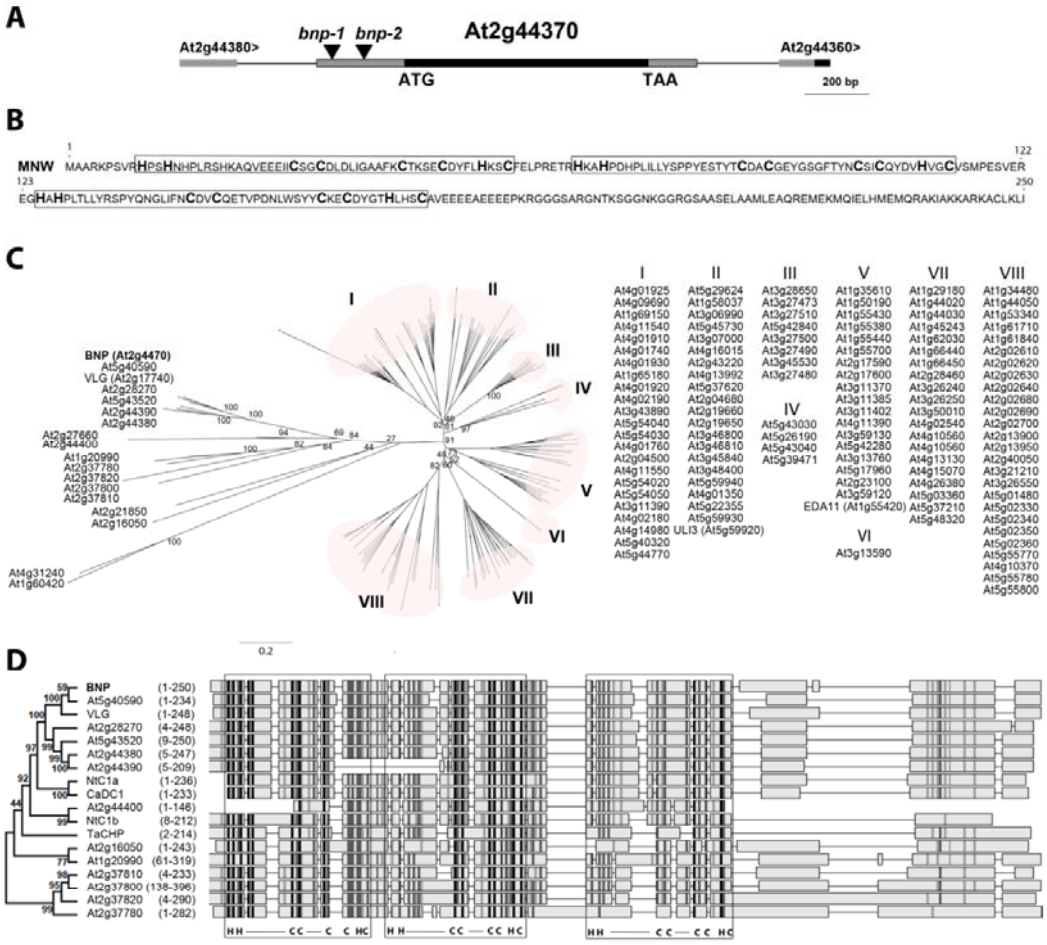

Figure 1. *BNP* codes for a DC1 domain containing protein. (A) Schematic view of a region of Arabidopsis chromosome 2 (from 18,323,538 to 18,321,537 bp -TAIR10) showing *BNP* genomic location and *bnp-1* and *bnp-2* insertion sites. (B) BNP amino acid sequence with boxed DC1 domains. (C) Phylogenic tree of 140 DC1 domain containing proteins in Arabidopsis. Bootstrap test results (1000 replicates) of the major nodes are indicated. IDs of sequences grouped in clusters I to VIII are listed. (D) Alignment of BNP with its closest Arabidopsis homologs and CaDC1 (AEI52549), TaCHP (ACU80555), NtDC1a (BAF80452) and NtDC1b (BAF80453). Phylogenic tree with bootstrap test results (1000 replicates) for the alignment of the complete 18 sequences is shown. Amino acid region represented for each sequence is indicated. DC1 domains are framed, signature residues and binding loop regions are indicated (C=Cys, H=His, — = loop). Higher intensity in grey scale denotes higher sequence similarity.

between *bnp/BNP* and WT plants and calculated the transmission efficiency of the mutant allele (TE = resistant/WT offspring x 100) (Table 1). Only 15.5% of microgametophytes carrying *bnp-1* and 22.0 % of the microgametophytes carrying *bnp-2* transmitted the insertion to the next generation ($p<0.0001$, Chi square test), indicating that *bnp* affects male gametophyte development or function (Table 1). No significant defects were observed for transmission through the female gametophyte (90.8% and 95.9% for *bnp-1* and *bnp-2*, respectively, table 1, p-values 0.51 and 0.66 respectively, Chi-square test).

Although the insertions in *BNP* compromised the transmission of the mutation through the male gametophyte, a fraction (about 15-22%) of pollen grains might still be able to transmit the insertion to the next generation. However, we did not recover homozygous mutant plants in the self-progeny of hemizygous plants. Thus, we investigated whether embryogenesis or germination were affected by the mutation analyzing pistils and seeds from *bnp/BNP* plants. No obvious embryo defects were observed in siliques from *bnp/BNP* plants, as neither developing siliques nor seed sets showed differences from WT siliques (Fig. S1). However, seeds from *bnp/BNP* self-pollinated plants showed reduced germination rates when compared to WT plants (94.8% for *bnp-1/BNP* (*n* = 754), 93.3% for *bnp-2/BNP* (*n* = 973) and 98.9% for WT (*n* = 440)). Further analysis of the germinated seeds showed that a fraction of the seedlings arrested soon after germination. Values of seedling lethality obtained were of 0.9% for WT (*n* = 440), 3.4% (*n* = 754) for seeds from *bnp-1/BNP* self-pollinated plants and 4.5% (*n* = 973) for *bnp-2/BNP* self-pollinated plants (Table 2). PCR genotyping of arrested seedlings showed that 75% (*n* = 12) corresponded to *bnp/bnp* homozygous individuals.

Altogether these results suggest that the mutation might cause impairment in male gametogenesis or function, reduced seed germination and seedling lethality, which combined, explain the absence of homozygous mutant plants in the progeny of selfed hemizygous plants.

Pollen development in *bnp* mutants is arrested at the binuclear stage

Viability of mature pollen was analyzed in *bnp-1* and *bnp-2* by means of Alexander staining and FDA staining. No differences were observed compared to pollen obtained from WT plants, indicating that the *bnp* mutation does not affect pollen viability (Fig. S2).

We later analyzed nuclear composition of mature pollen using DAPI staining. Normal mature pollen contains three nuclei: a vegetative nucleus and two sperm nuclei generated by the mitotic division of the generative nucleus. Mature pollen from WT plants showed 99.2% (*n* = 772) of trinucleate grains. On the other hand, *bnp/BNP* plants presented only about 57-59% of trinucleate mature pollen grains (56.9% (*n* = 1123) in *bnp-1/BNP* and 59.0% (*n* = 981) in

195 *bnp-2/BNP*). The rest were found in a binucleate stage, suggesting
196 developmental arrest.

197 A genetic complementation assay confirmed that the insertions in *BNP*
198 are causing the abnormalities observed during pollen development. *bnp-1/BNP*
199 hemizygous plants transformed with a *ProBNP:BNP:GFP* translational fusion
200 construct showed trinucleate mature pollen grains at similar levels of WT plants
201 (Fig. S3). This result was recorded in T3 plants of five independent
202 complemented lines.

203 In order to better characterize the defect observed during pollen
204 development, *bnp-1/BNP* plants were crossed to *qrt1* homozygous plants,
205 which are impaired in a pectin methyl esterase responsible for the separation of
206 microspores tetrads (Francis et al., 2006). F2 plants that carried the insertion in
207 *BNP* in hemizygosis and were homozygous for *qrt1* (*bnp/BNP qrt1/qrt1*) were
208 further analyzed. Mature tetrads were collected and stained with DAPI.
209 Consistently with our previous results, most tetrads of *bnp-1/BNP qrt1/qrt1*
210 plants showed an abnormal number of nuclei (Fig. 2A), indicating a failure to
211 complete PMII in about 46% of the pollen grains analyzed.

212 We next assessed germination of pollen grains in the tetrads. As shown
213 in Fig. 2, germination rates were 37.7% in pollen collected from *bnp-1/BNP*
214 *qrt1/qrt1* plants and 68.2% in pollen grains from *BNP/BNP qrt1/qrt1* plants (Fig.
215 2F). This indicates a reduction of 44.7% in the germination rate in pollen from
216 *bnp-1/BNP qrt1/qrt1* plants compared to pollen grain tetrads from *BNP/BNP*
217 *qrt1/qrt1* plants. As the reduction in the rate of germination observed in the
218 hemizygous background *bnp-1/BNP* was less than 50%, this suggests that
219 although severely affected, a small fraction of *bnp* pollen grains is still able to
220 germinate.

221 Analysis of pollen grain germination in *bnp-2/BNP* plants showed
222 comparable values, as we calculated a decrease in germination rate of about
223 36% compared to pollen grains from WT plants. Germination rates of 43% (n =
224 787) and 67% (n = 443) were recorded for pollen grains collected from *bnp-*
225 2/BNP and WT plants respectively.

A

Genotype	Observed nuclear phenotype			
	Four trinucleate (image B)	Three trinucleate, one binucleate (image C)	Two trinucleate, two binucleate (image D)	Two trinucleate, one tetranucleate (image E)
BNP/BNP	96.9 % (187/193)	3.1 % (6/193)	0 % (0/193)	0 % (0/193)
bnp-1/BNP	0.9 % (2/229)	11.8 % (27/229)	83.4 % (191/229)	3.9 % (9/229)

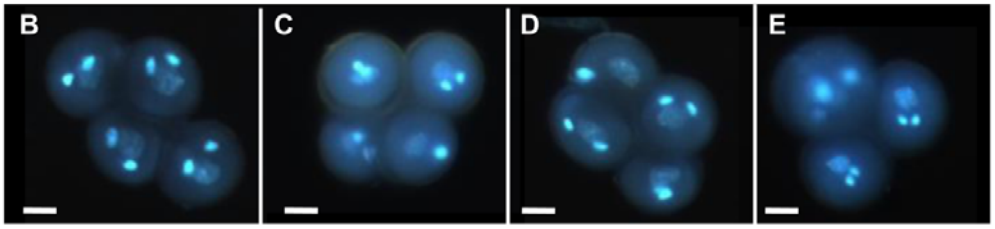

F

Genotype	Pollen germination rate	Observed tetrad phenotype				
		Four germinated (image G)	Three germinated (image H)	Two germinated (image I)	One germinated (image J)	none germinated (image K)
BNP/BNP	68.2 % (573/840)	35.2 % (74/210)	35.6 % (75/210)	10.5 % (22/210)	5.7 % (12/210)	12.8 % (27/210)
bnp-1/BNP	37.7 % (291/772)	0% (0/193)	8.8 % (17/193)	46.6% (90/193)	31.1 % (60/193)	13.4 % (26/193)

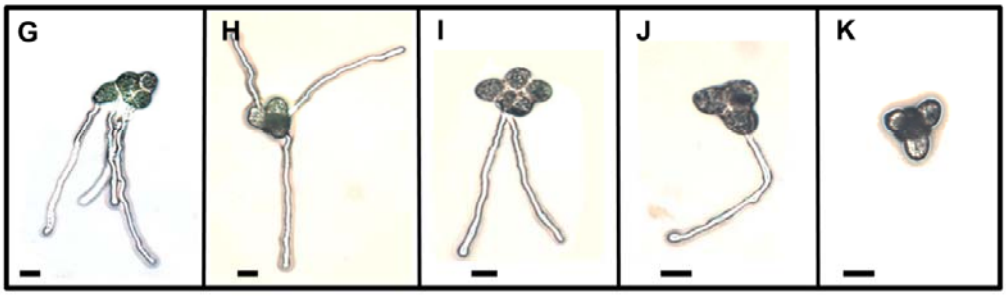

Figure 2. Pollen development and germination is impaired in *bnp-1* mutants. (A) Quantification of phenotypes observed in *BNP/BNP* and *bnp-1/BNP* plants in *qrt1/qrt1* background. (B-E) Nuclear configuration types revealed by DAPI (4',6-Diamidino-2-phenylindole) staining. Bars = 10 µm (F) Quantification of pollen tube germination in tetrads from *BNP/BNP* and *bnp-1/BNP* plants in *qrt1/qrt1* background. (G-K) Types of pollen tube germination in tetrads. Bars = 20 µm.

These results showed that *BNP* is required to complete pollen development, specifically to undergo PMII. Arrested pollen grains were viable, but germination was impaired, which explains the reduced transmission of *bnp* through the male gametophyte (Table 1).

BNP is expressed in pollen and young sporophytic tissues

Expression of *BNP* was studied in Arabidopsis plants expressing the *BNP-GFP* fusion driven by the *BNP* promoter, which was proved to be functional, as it complemented the phenotype in *bnp/BNP* plants (Fig. S3). BNP-GFP was detected in cytoplasmic speckles following a punctuate pattern at early stages of pollen development (microspore tetrad and released microspore) and in discrete bigger compartments at bicellular and tricellular stages (Fig. 3A and 3H). The same expression pattern was observed in the pollen tube (PT) of germinating pollen grains (Fig. 3I-J).

To gain further knowledge of BNP roles *in planta*, a reporter construction expressing the *GUS* gene under the control of *BNP* promoter was used to analyze *BNP* expression. GUS activity accumulated at early stages of seedling development, mainly in vascular tissues and developing leaves. It was also observed associated to anthers at very early stages of floral development, indicating that expression of *BNP* can be detected before meiosis (Fig. 3K-S). Expression data observed were comparable to transcriptional data available in the efp Browser Data Analysis Tool (https://bar.utoronto.ca/eplant/) (Fig. S4). These results also indicated that BNP could be functional not only during pollen development but also at additional developmental stages, such as sporogenesis, germination and early stages of sporophyte development.

BNP interacts with transcription factors VOZ1 and VOZ2

To gain insight into possible functions of BNP we carried out a yeast-two-hybrid screening to identify potential BNP protein interactors. Two closely related NAC family transcription factors, VOZ1 and VOZ2, were identified among interactors (a selection of the identified clones is presented in Table S1). Interestingly, VOZ1 and VOZ2 were reported to bind a pollen-specific promoter element (Mitsuda et al., 2004). BNP was also retrieved in the Y2H screening as a self-interactor (Table S1). To confirm BNP-VOZ1, BNP-VOZ2 and BNP-BNP interactions, we performed Bimolecular Fluorescence complementation (BiFC) assays.

We made constructs to express BNP and each of the candidate proteins fused either to the N- or the C-terminal of yellow fluorescent protein (YFP) fragments to generate BNP-N-YFP and VOZ1-C-YFP, VOZ2-C-YFP or BNP-C-

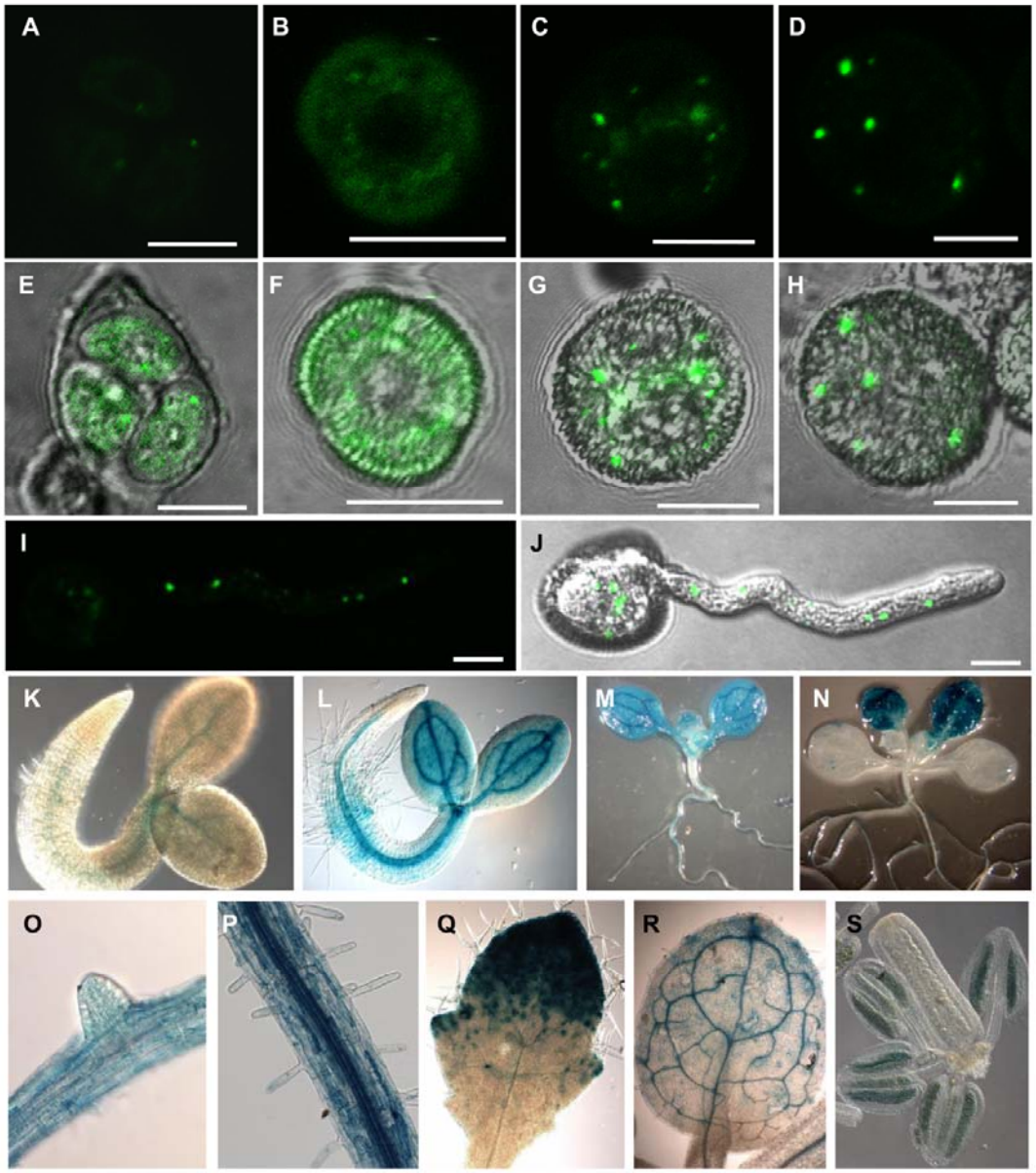

Figure 3. *BNP* is expressed in pollen and young sporophytic tissues. (A-D) Confocal images showing BNP-GFP through microgametogenesis. (E-H) Overlay between DIC and GFP fluorescence. (A and E) Microspore tetrad, (B and F) released microspore, (C and G) bicellular stage and (D and H) tricellular stage. (I) Image showing a projection along the z axis of all planes showing GFP fluorescence. (J) overlay of DIC and GFP fluorescence showing a germinating pollen grain. (K-S) GUS activity in Arabidopsis transgenic plants carrying the *pBNP:GUS* construct. (K) Seedling 24 h after imbibition, (L) 48 h after imbibition, (M) 6 days post germination and (N) 12 days post germination. (O) Root with lateral root primordium, (P) primary root with root hairs, (Q) third leaf 8 days after imbibition (R) third leaf 14 days after imbibition. (S) GUS signal was detected inside anthers at floral developmental stage 10. Three independent transgenic lines were used for this study. Pictures are representative of the results obtained in all analyzed lines. Bars = 10 µm.

YFP fusion constructs. The fusion constructs under control of the CaMV 35S promoter were used to transiently transform *N. benthamiana* leaves and BiFC signals were analyzed using confocal microscopy (Fig. 4). YFP was detected following a punctate pattern indicating BNP interaction with VOZ1, VOZ2 and with itself (Fig. 4). Control *N. benthamiana* leaves transfected either with BNP-

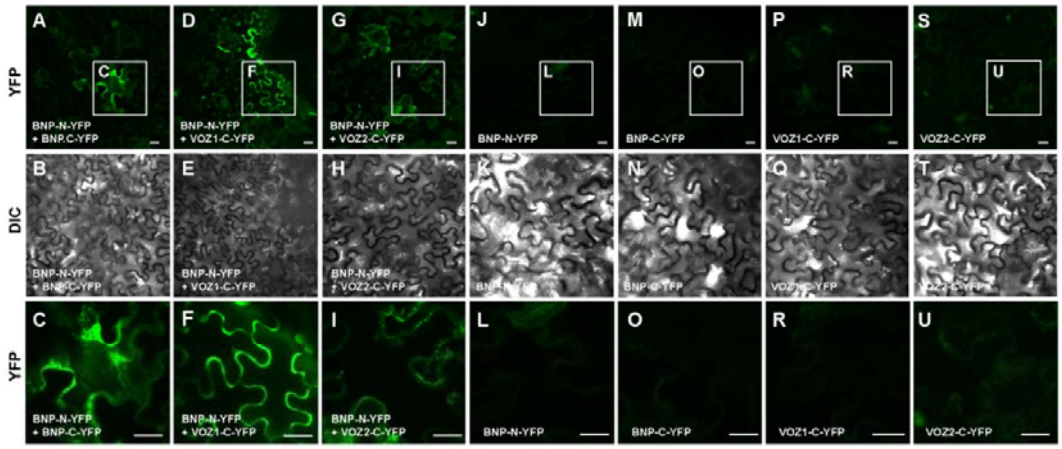

Figure 4. BNP interacts with itself, VOZ1 and VOZ2. Bimolecular fluorescence complementation (BiFC) analysis of the interaction of BNP with itself, VOZ1 and VOZ2 in *Nicotiana benthamiana* leaves. Representative confocal microscopy images showing that BNP interacts with (A–C) itself, (D-F) VOZ1 and (G-I) VOZ2. Reconstituted YFP fluorescence (YFP) or DIC images of *N. benthamiana* leaves are shown in epidermal cells co-infiltrated with *Agrobacterium tumefaciens* harboring the indicated constructs. Control *N. benthamiana* leaves transfected with (J-L) BNP-N-YFP, (M-O) BNP-C-YFP, (P-R) VOZ1-C-YFP, (S-U) VOZ2-C-YFP do not show any BiFC signal. The last row (C, F, I, L, O, R, U) correspond to the magnification of regions of interest (insets) indicated in the first row. Bars = 20 µm.

N-YFP, VOZ1-C-YFP, VOZ2-C-YFP or BNP-C-YFP did not show any BiFC signal (Fig. 4). An additional control experiment using VLG (as BNP closest homolog, sharing 72.0% identity) showed negative results with VOZ1, VOZ2 and BNP indicating the specificity of the observed interactions (Fig. S5).

BNP mainly localizes to prevacuolar compartments and co-localizes with VOZ1 and VOZ2

We used the lipophilic dye FM4-64 to gain insight on the subcellular localization of BNP. After internalization, this dye is sequentially distributed to different organelle membranes, following the endocytic pathway (Bolte et al., 2004). We followed FM4-64 in roots of plants expressing the fusion protein BNP-GFP at different time points. We observed no co-localization of internalized FM4-64 and BNP-GFP after 30 min to 2 h of incubation (Fig. S6), discarding localization of BNP-GFP to early endosomes or to components of the *trans*-Golgi Network. In agreement with that, BNP-GFP did not co-localize with Brefeldin bodies caused by the addition of the endosomal recycling inhibitor Brefeldin A to FM4-64 treated roots (Fig. S6).

To assess BNP localization, we used *N. benthamiana* to transiently express BNP-GFP together with a prevacuolar compartments marker, the Rab5 GTPase Rha1 fused to RFP (Foresti et al., 2010) or with a Golgi apparatus

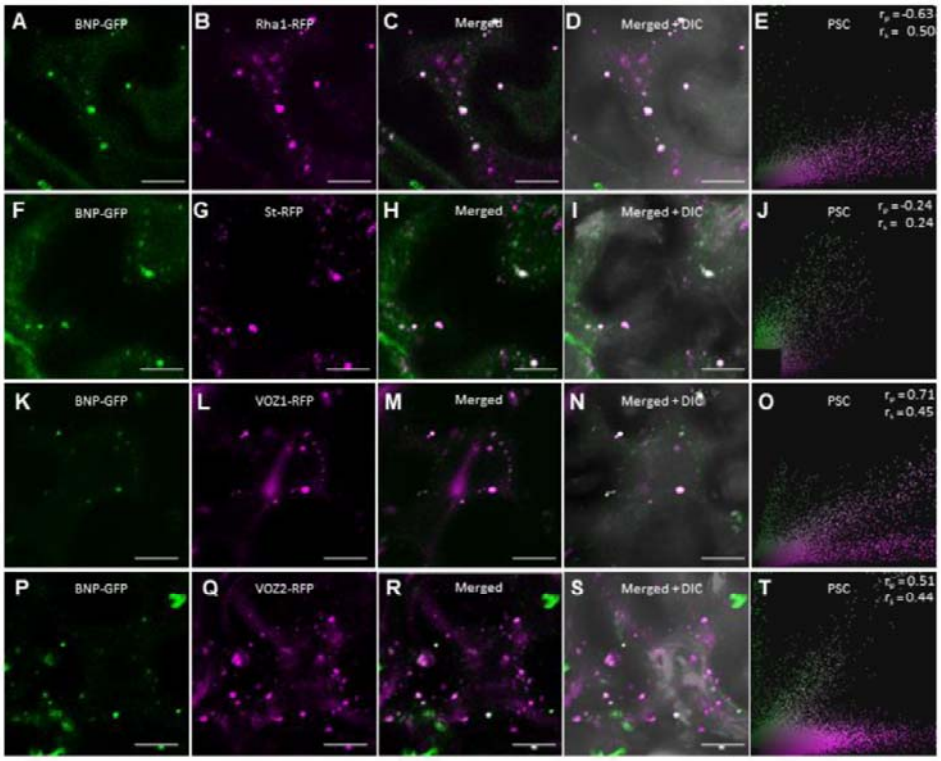

Figure 5. BNP co-localizes with VOZ1 and VOZ2 to prevacuolar compartments. (A, F, K and P) Localization of BNP-GFP transiently expressed in *Nicotiana benthamiana* epidermal cells. (B) Fluorescent marker for prevacuolar compartments, RFP-Rha1. (C) Merged image of BNP-GFP and RFP-Rha1. (D) Shows an overlay with the corresponding bright-field image. (E, J, O and T) Pearson and Spearman correlation (PSC) test calculated using a plugin for ImageJ; r values indicate the level of co-localization ranging from +1 for perfect co-localization to −1 for negative correlation. (G) Fluorescent marker for Golgi apparatus, St-RFP. (H) Merged image of BNP-GFP and St-RFP. (I) Shows an overlay with the corresponding bright-field image. (L) Localization of RFP-VOZ1. (M) Merged image of BNP-GFP and RFP-VOZ1. (N) Shows the corresponding bright field image of the cells showed in (M). (Q) Localization of RFP-VOZ2. (R) Merged image of BNP-GFP and RFP-VOZ2. (S) Bright field image of the cells showed in (R). Bars = 20 µm.

marker, the rat sialyltransferase St fused to RFP (Wee et al., 1998). Representative images shown in Fig. 5 and Pearson and Spearman correlation (PSC) values indicated that BNP-GFP co-localized with Rha1-RFP (Fig. 5A-E) and did not co-localize with St-RFP (Fig. 5F-J), suggesting that BNP is mainly confined to prevacuolar compartments associated vesicles.

To further confirm that BNP and VOZ proteins are indeed localized in the same subcellular compartment, we performed a co-localization study. *N. benthamiana* plants were transiently co-transfected with constructions to express BNP-GFP and either VOZ1-RFP or VOZ2-RFP. In these transfected cells, a typical punctuate expression was detected for BNP-GFP and high levels

of co-localization were observed with both, VOZ1-RFP and VOZ2-RFP (Fig. 5K-T).

BNP is required for nuclear localization of VOZ1 in pollen

Since VOZ1 and VOZ2 do not contain neither a transmembrane region nor signals that can predict their subcellular confinement, we analyzed a possible role for BNP on VOZ protein localization in pollen from WT and *bnp* plants.

To test this, we transformed *BNP/BNP* and hemizygous *bnp-1/BNP* plants, both in the *qrt1* background, with *ProUb10:VOZ1-RFP* and analyzed VOZ1-RFP intracellular localization during pollen development (Fig. 6). The introduction of the mutation in the *qrt1* background allows to compare and analyze any difference in VOZ1 localization that might arise from an impairment in BNP, as pollen tetrads of the *bnp-1/BNP* genotype are constituted by two mutant (binucleate) and two WT (trinucleate) pollen cells.

At earlier developmental stages (microspore and bicellular pollen) VOZ1 was detected at the cytoplasm with very low signal intensities, showing no differences between *qrt1/qrt1*, *BNP/BNP, VOZ1-RFP* and *qrt1/qrt1*, *bnp-1/BNP, VOZ1-RFP* genotypes. (Fig. 6A-H). In mature WT pollen, however, VOZ1-RFP was detected at higher levels and its localization appeared distributed between the cytoplasm and the nuclei. Most of the pollen tetrads (91.5%) from *qrt1/qrt1*, *BNP/BNP, VOZ1-RFP* plants presented VOZ1 nuclear localization in the four cells of the tetrad (Fig. 6M). However, most of the tetrads from the *qrt1/qrt1*, *bnp-1/BNP,* VOZ1-RFP genotype presented VOZ1 nuclear localization only in one or two pollen cells (85.2%, Fig. 6M).

Next, we analyzed if the lack of a functional BNP could also affect the levels of VOZ1 in pollen. We quantified VOZ1-RFP by measuring red fluorescence intensity in mature pollen cells of *qrt1/qrt1*, *bnp-2/BNP,* VOZ1-RFP and *qrt1/qrt1*, *bnp-2/BNP,* VOZ1-RFP plants (Fig. S9). Interestingly, lower red fluorescence levels were recorded in *qrt1/qrt1, bnp-2/BNP,* VOZ1-RFP plants suggesting that BNP could have a role in the promotion of VOZ1 stabilization.

Altogether, these results strongly suggest that BNP is involved in VOZ1 localization, as its nuclear localization relies on the presence of a functional BNP.

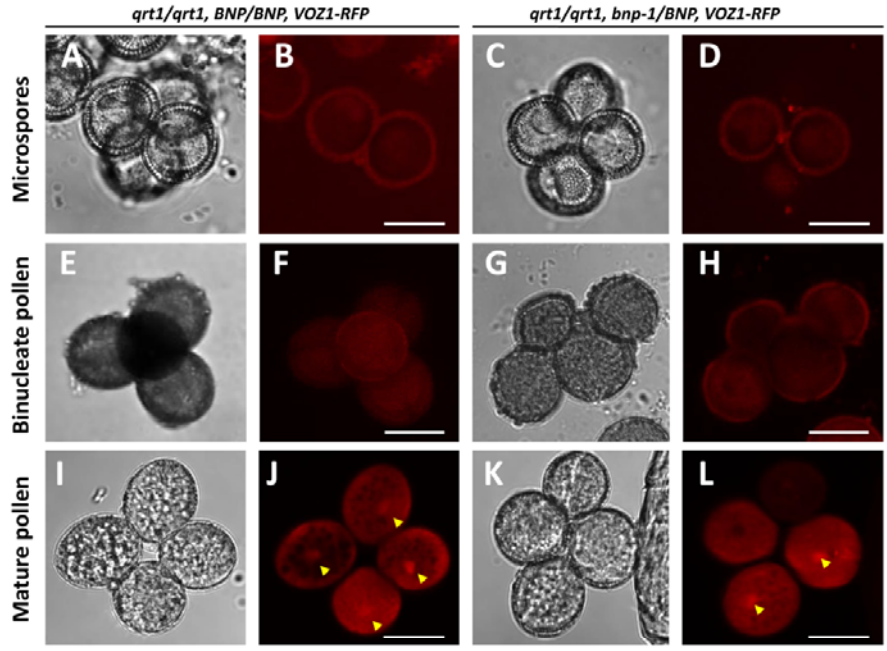

M

Genotype	Observed VOZ1 localization				
	Four nuclear	Three nuclear, one cytoplasmic	Two nuclear, two cytoplasmic	One nuclear, three cytoplasmic	Four cytoplasmic
qrt1/qrt1, BNP/BNP, VOZ1-RFP	91.5 % (65/71)	7.0 % (5/71)	1.4 % (1/71)	0 % (0/71)	0 % (0/71)
qrt1/qrt1, bnp-1/BNP, VOZ1-RFP	1.3 % (1/76)	11.8 % (9/76)	57.8% (44/76)	27.6% (21/76)	1.3 % (1/76)

N

Genotype	Observed nuclear phenotype			
	Four trinucleate	Three trinucleate, one binucleate	Two trinucleate, two binucleate	Two binucleate, one tetranucleate
qrt1/qrt1, BNP/BNP, VOZ1-RFP	97.3 % (71/73)	2.7 % (2/73)	0 % (0/73)	0 % (0/73)
qrt1/qrt1, bnp-1/BNP, VOZ1-RFP	3.6 % (4/110)	18.2 % (20/110)	77.3 % (85/110)	0.9 % (1/110)

Figure 6. Nuclear localization of VOZ1 is affected in *bnp* mutants.
Pollen tetrads from *qrt1/qrt1, BNP/BNP, VOZ1-RFP* (A, B, E, F, I, J) and *qrt1/qrt1, bnp-1/BNP, VOZ1-RFP* (C, D, G, H, K, L) plants were analyzed at microspore (A-D), binucleate (E-H) and mature tricellular (I-L) stages. Representative z-stack images of confocal micrographs displaying VOZ1-RFP fluorescence (B, D, F, H, J, L) and bright field images (A, C, E, G, I, K) are shown. Arrowheads indicate nuclear localized VOZ1. Bars = 10 µm.
Mature pollen tetrads from four *qrt1/qrt1, BNP/BNP, VOZ1-RFP* and three *qrt1/qrt1, bnp-1/BNP, VOZ1-RFP* plants were analyzed by fluorescent microscopy and VOZ1 localization (M) and nuclear configuration (N) were scored. Observed number and total pollen tetrads are indicated in parenthesis.

We later analyzed BNP localization during pollen development using WT plants harboring stable *BNP-GFP* and *VOZ1-RFP* constructs. We observed that both, VOZ1 and BNP, localized in the cytoplasm at early developmental stages. Contrasting VOZ1, no nuclear localization was recorded for BNP (Fig. S9). Partial co-localization was detected in areas in the cytosol were BNP and VOZ1 might interact at microspore and bicellular stages. This was not observed in mature pollen, where VOZ1 show both nuclear and cytoplasmic localization. As BNP remained in the cytosol at every developmental stage, forming speckles during binucleate and mature pollen stages, any role related to VOZ proteins

343 translocation/function would be carried out outside the nucleus and before
344 pollen maturation.
345
346
347

DISCUSSION

In this study we identified *BNP*, a gene coding for a DC1 domain protein that is required for pollen development and germination. Analysis of hemyzigous *bnp/BNP* plants showed that transmission through the male gametophyte is severely impaired; about half of pollen grains from *bnp/BNP* plants resulted arrested at PMII stage and their germination was significantly reduced.

By means of Y2H and BiFC experiments, we identified and confirmed VOZ1 and VOZ2 as BNP interacting proteins. VOZ1 and VOZ2 are transcription factors that belong to the NAC transcription factor family, and were reported as involved in the control of flowering time (Celesnik et al., 2013; Yasui and Kohchi, 2014), either through the binding of PhyB (Yasui et al., 2012), Flowering Locus C (Mimida et al., 2011) or Constans (Koguchi et al., 2017; Kumar et al., 2018). VOZ proteins were also related to biotic and abiotic stress responses (Nakai et al., 2013; Song et al., 2018; Schwarzenbacher et al., 2020; Wang et al., 2021). VOZ1 and VOZ2 were proved to be functionally redundant, as single mutants for each gene showed normal phenotypes, but *voz1voz2* double mutants displayed phenotypic defects (Yasui et al., 2012; Celesnik et al., 2013; Nakai et al., 2013; Kumar et al., 2018). Interestingly, these plants presented the same pollen developmental defect observed in *bnp/BNP* plants, as a fraction of *voz1voz2* pollen grains contained only two nuclei –the vegetative nucleus and a single reproductive nucleus (Celesnik et al., 2013). This fact supports a physiological role for the interaction between BNP and VOZ proteins during pollen development.

BNP was localized mainly to PVC, in Rha1 positive vesicles. VOZ proteins are functional in the nucleus, but they were initially identified in cytoplasmic speckles and a cytoplasmic-nuclear translocation was proposed to modulate VOZ activity as transcriptional regulators (Yasui et al., 2012; Koguchi et al., 2017). VOZ1 and VOZ2 do not contain neither a transmembrane region nor localization signals such as NLS or NES (Jensen et al., 2010). This suggests that VOZ1 and VOZ2 nuclear/cytoplasmic localization must rely on another mechanism. Endocytic proteins have been previously shown to participate in the spatiotemporal regulation of transcription factors (Palfy et al., 2012; Wu et al., 2012; Serrano et al., 2016). They may facilitate the assembly of multi-molecular complexes through protein–protein interaction domains and act

as regulators (Pyrzynska et al., 2009). As can be concluded from the analysis showed in Fig. 6 and Table 3 a similar situation could be taking place between the pairs BNP-VOZ1, where BNP is required for VOZ1 nuclear localization. Implications of VOZ1/2 nuclear translocation may be related to VOZ1/2 role as a transcriptional regulator, as it was proposed to be exerted in the nucleus (Yasui et al., 2012). Interestingly, VOZ proteins nuclear localization was rarely detected, and the addition of NLS signals was usually required to place it the nucleus (Yasui et al., 2012).(Schwarzenbacher et al., 2020) However it was reported that degradation of VOZ1/2 takes also place in the nucleus, facilitated by the E3 ubiquitin ligase BRUTUS (Selote et al., 2018). Thus, BNP role could be involved in the function and/or in the degradation of VOZ1/2.

Our results also indicated that BNP could be essential not only during pollen development but also at additional developmental stages, such as germination and early stages of sporophyte development. In agreement with this, *BNP* expression was detected very early during seedling development, in particular in vascular tissues (Fig. 3). The expression pattern of BNP also suggests that it could play roles in other sporophytic tissues, either through the interaction with VOZ TFs, that are also ubiquitously expressed through the plant (Yasui et al., 2012), or through the interaction with other proteins. Potential BNP interacting proteins identified by Y2H experiments (Supplemental Table S2) provide a promising list of candidates that might be involved with BNP function in other plant tissues.

Only one additional DC1 domain protein, VLG, has been characterized so far and was likewise proved to be required for pollen development. However, *VLG* deficiency caused microgametogenesis arrest at PMI, an earlier stage, yielding unviable uninucleate pollen grains (D'Ippólito et al., 2017). On the other hand, VLG was also essential for female gametogenesis (D'Ippólito et al., 2017).

Notably, the Arabidopsis genome encodes for over 140 uncharacterized proteins harboring DC1 domains. Multiple sequence alignments of DC1 domain proteins from different species showed amino acid conservation restricted to the residues that define the DC1 signature motif, but divergence in the amino acids corresponding to the folded domain -which might define binding capabilities (Rahman and Das, 2015)- suggesting a diversity of interactors. Thus, DC1

domain proteins emerge as a novel family of highly specialized modular scaffold proteins, capable to promote the recruiting of binding targets and affect their localization and functionality.

Altogether, our results support a role for BNP acting as a scaffold protein recruiting VOZ1 and VOZ2 to prevacuolar compartments. This recruitment appears to facilitate VOZ1 -and likely VOZ2- translocation to the nucleus, promoting their activity as transcriptional regulators during pollen development. In addition, a role of BNP in the regulation of the levels VOZ proteins could not be discarded, as lower levels of these proteins were present in mature pollen lacking a functional BNP.

MATERIALS AND METHODS

Plant materials and growth conditions

Arabidopsis (Columbia [Col-0] ecotype) lines SALK_114889 (*bnp-1,* with T-DNA insertion located in chr2 TAIR10 18,323,075) and GK-008E01 (*bnp-2,* with T-DNA insertion located in chr2 TAIR10 18,323,371) were obtained from ABRC (Ohio State University, Ohio, USA) (Alonso et al., 2003). Both lines were backcrossed twice to the WT Columbia prior to their use. Single insertion in At2g44370 after backcrosses and all genotypes were confirmed by PCR-based genotyping and segregation analysis. When indicated seeds were sterilized in 20% (v/v) sodium hypochlorite, washed with sterile water and plated on MS plates with 50 µg/mL kanamycin or 7.5 µg/mL sulfadiazine, stratified at 4°C for 48 h and placed at 23°C, 16 h light, 8 h dark. Resistant seedlings were then transferred onto soil and grown under the conditions described above.

Molecular characterization of insertional lines

For *bnp-1*, the left border–genomic sequence junction was determined by PCR in plants showing kanamycin resistance using the T-DNA-specific primer LBb1 combined with the genomic sequence specific primers bnp-1 RP and bnp-1 LP (Table S1). For *bnp-2*, the left border–genomic sequence junction was determined by PCR in plants showing sulfadiazine resistance using the T-DNA–specific primer GKGT8474 combined with the genomic sequence specific primers bnp-2 RP and bnp-2 LP (Table S1).

Segregation Analysis

For self-cross analysis, the progeny of self-pollinated hemizygous plants was germinated on selective growth medium containing 50 µg/mL kanamycin for *bnp-1* or 7.5 µ/mL sulfadiazine for *bnp-2*, and the ratio of resistant to sensitive plants was scored. Reciprocal crosses were performed as described previously (Pagnussat et al., 2005).

Constructions

Genomic DNA was extracted from rosette leaves or whole seedlings as described (León et al., 2007). To generate *ProBNP:BNP-GFP* translational fusion the region including *BNP* ORF and putative promoter (672 upstream the ATG codon) was amplified by PCR using the primer combination listed in Table S1. The amplicon was cloned using pENTR™ Directional TOPO® Cloning Kit (Invitrogen) using Gateway® technology and the sequence was verified. The resulting plasmid *pENTR-ProBNP-BNP* was subjected to the LR reaction using the destination vector pMDC107 (Curtis and Grossniklaus, 2003). The *ProBNP:GUS* construct was generated amplifying the *BNP* putative promoter region (672 upstream the ATG codon) by PCR using the primer combination listed in Table S1. The amplicon was cloned into pENTR™/TOPO (Invitrogen) and its sequence was verified. The resulting plasmid *pENTR-ProBNP* was subjected to the LR reaction using the destination vector pMDC162 (Curtis and Grossniklaus, 2003). For *Pro35S:BNP-GFP* construct, *BNP* ORF was PCR amplified using as template clone DKLAT2G44370 obtained from ABRC (Ohio State University, Ohio, USA) using the primer combination listed in Table S1. The amplicon was cloned into pENTR™/TOPO (Invitrogen) and its sequence was verified. The resulting plasmid *pENTR-BNP* was subjected to the LR reaction using the destination vector pMDC83 (Curtis and Grossniklaus, 2003). For *ProUb10:VOZ1-RFP* and *ProUb10:VOZ2-RFP* constructions, respective ORFs were PCR amplified using primers listed in Table S1, cloned in pENTR™/TOPO (Invitrogen) and sequence-verified. The resulting plasmids *pENTR-VOZ1* and *pENTR-VOZ2* were subjected to the LR reaction using the destination vector pUBN-RFP-DEST (Grefen et al., 2010).

Obtaining *bnp/BNP* plants in the *qrt1* background

To obtain *bnp* mutants in *qrt1* background, *bnp-1/BNP* was crossed with *qrt1* homozygous plants. Kan resistant plants from the progeny were selected and allowed to self-fertilize. Homozygous *qrt1* plants harboring *bnp* mutations were selected for further analysis (Johnson-Brousseau and McCormick, 2004).

In a similar way, *qrt1/qrt1-bnp-2/BNP*-VOZ1-RFP plants were obtained crossing *bnp-2/BNP* plants expressing VOZ1-RFP with *qrt1* homozygous plants.

Transformation of Agrobacterium tumefaciens and Arabidopsis

Vectors were introduced into Agrobacterium strain GV3101 by electroporation. Arabidopsis WT plants were transformed using the floral dip method (Clough and Bent, 1998). Transformant plants were selected based on their ability to survive in MS medium with 15 mg. L^{-1} hygromicyn. Resistant (green seedlings with true leaves) were then transferred to soil and grown under the conditions described above.

Morphological and histological analyses

Pollen grains viability was assessed using Alexander's staining (Alexander, 1969) and fluorescein diacetate (FDA) staining (Heslop-Harrison and Heslop-Harrison, 1970). For pollen development analysis, successive buds in the same inflorescence were collected (Lalanne and Twell, 2002), fixed in ethanol:acetic acid 3:1 until discoloration and stored at room temperature. Anthers were washed, dissected and mounted on microscopy slides with DAPI staining solution. For pollen tube germination, pollen grains were incubated overnight in a dark moisture chamber at 22°C in 0.01% boric acid, 5mM $CaCl_2$, 5mM KCl, 1 mM $MgSO_4$, 10% sucrose pH 7.5 and 1.5% agarose, as described previously (Boavida and McCormick, 2007). For GUS staining, tissues from *ProBNP:GUS* carrying plants were collected and incubated in GUS staining solution as already described (Pagnussat et al., 2007). Gametophytes were observed on a Zeiss Axio Imager A2 microscope using DIC optics. Seedlings were observed on a Nikon SMZ800 Stereomicroscope and images were captured with a Canon DS126431 camera.

Co-localization experiments in *Nicotiana benthamiana*

A. tumefaciens strain GV3101 carrying *Pro35S:BNP-GFP* was co-infiltrated with *A. tumefaciens* cells carrying either the late endosome marker *RFP-Rha1* or the Golgi apparatus marker *St-RFP*, in leaf epidermal cells of *N. benthamiana* plants. Infiltrated leaves were analyzed 48-72 h after infiltration on a confocal microscope (Nikon Eclipse C1 Plus) using EZ-C1 3.80 imaging software and Ti-Control. Pearson and Spearman correlation (PSC) plugin for ImageJ was used to calculated correlation coefficients from a minimum of 400 individual punctae from at least 10 independent cell images (French et al., 2008).

Yeast two-hybrid screen

The Y2H screening was performed by Hybrigenics Services S.A.S. (Paris, France). A DNA fragment encoding Arabidopsis At2g44370 (amino acids 1-250) was PCR-amplified and cloned into pB66 as C-terminal fusion to Gal4 DNA-binding domain (Gal4-At2g44370) and used as a bait to screen Universal Arabidopsis Normalized library containing 3.2 million of independent clones in pGADT7-RecAB vector. pB66 derive from the original pAS2ΔΔ (Fromont-Racine et al., 1997). For the Gal4 bait construct, 35 million clones were screened using a mating approach with YHGX13 (Y187 ade2-101::loxP-kanMX-loxP, matα) and L40ΔGal4 (mata) yeast strains as previously described (Fromont-Racine et al., 1997). 158 His+ colonies were selected on a medium lacking tryptophan, leucine and histidine. The prey fragments of the positive clones were amplified by PCR and sequenced at their 5' and 3' junctions. The resulting sequences were used to identify the corresponding interacting proteins in the GenBank database (NCBI) using a fully automated procedure. A confidence score (PBS, for Predicted Biological Score) was attributed to each interaction as previously described (Formstecher et al., 2005).

Bimolecular fluorescence complementation (BiFC) analysis

The cDNA sequences of At2g44370 (*BNP*), At1g28520 (*VOZ1*), At2g42400 (*VOZ2*) and At2g17740 (*VLG*) were PCR amplified using the primers listed in Table S1. The PCR products were cloned into pENTR^{TM}/TOPO (Invitrogen), sequenced and recombined through BP reaction into BiFC destination plasmids pUBN-YN and pUBN-YC (Grefen et al., 2010). The binary plasmids were then

transformed into *A. tumefaciens* strain GV3101 by electroporation. Split nYFP- and cYFP-tagged protein pairs and the gene-silencing suppressor p19 were co-expressed in *N. benthamiana* leaves by *A. tumefaciens* -mediated inoculation. Plant leaves were examined 48-72 h post-infiltration with a confocal microscope (Nikon Eclipse C1 Plus) using a Super Fluor 40.0x/1.30/0.22 Oil objective, numerical aperture 1.300. Acquisition was performed using EZ-C1 3.80 imaging software and Ti-Control. All pictures were acquired with the same settings.

Bioinformatics and phylogenetic analysis

Sequences from the DC1 domain family were identified using the Basic Local Alignment Search Tool (BLAST) from NCBI (National Center for Biotechnology Information) using initially BNP as a reference and retrieved sequences in iterative searches. Protein sequences alignments were performed using MEGA7 (version 7.0.14) (Kumar et al., 2016). Phylogenetic trees were constructed using the neighbor-joining method and the default settings of MEGA7 (version 7.0.14) (Kumar et al., 2016). The evolutionary distances were computed using the Poisson correction method (Zuckerkandl and Pauling, 1965) and are in the units of the number of amino acid substitutions per site. The trees were drawn using FigTree (version 1.4.3) (http://tree.bio.ed.ac.uk/). Graphic display of identities was visualized using Geneious (version 9.1.4) (http://www.geneious.com) based on an identity matrix (Kearse et al., 2012).

Accession Numbers

Sequence data from this article can be found in the Arabidopsis Genome Initiative database under accession numbers: BNP (At2g44370), VOZ1 (At1g28520), VOZ2 (At2g42400) and VLG (At2g17740).

Supplemental Data

Supplemental Figure S1. *bnp/BNP* hemizygous plants showed normal sporophytic phenotypes and seed sets.

Supplemental Figure S2. *bnp*/*BNP* hemizygous plants showed no differences in the viability of mature pollen.

582 **Supplemental Figure S3.** Complementation of *bnp-1/BNP* plants with
583 *ProBNP:BNP-GFP*.
584 **Supplemental Figure S4.** *BNP* expression in Arabidopsis
585 **Supplemental Figure S5.** BNP-related protein VLG does not interacts with
586 VOZ1, VOZ2 or BNP.
587 **Supplemental Figure S6.** Analysis of co-localization of BNP and the endocytic
588 tracer FM4-64
589 **Supplemental Figure S7.** Negative controls for co-localization experiments
590 showing positive correlations
591 **Supplemental Figure S8.** BPN and VOZ1 localization during pollen
592 development
593 **Supplemental Figure S9.** Quantification of VOZ1-RFP red fluorescence in
594 mature pollen of *qrt1/qrt1, BNP/BNP, VOZ1-RFP* and *qrt1/qrt1, bnp-1/BNP,*
595 *VOZ1-RFP* plants
596
597 **Supplemental Table S1.** Selected BNP interacting protein identified by a yeast
598 two-hybrid screening.
599 **Supplemental Table S2.** Primers used in the study
600

601 **Acknowledgements**
602 We would like to thank Michael Blatt and Christopher Grefen (Glasgow
603 University, UK) for providing pUB-Destination vectors, Jurgen Denecke
604 (University of Leeds, UK) for providing the constructs ST-RFP and Rha-RFP,
605 Nicolas Setzes for assistance with statistical analysis and Daniela Villamonte for
606 technical assistance with confocal microscopy. This research was funded by
607 grants to DFF from Agencia Nacional de Promoción Cientifica y Técnica
608 Argentina (PICT2013-1524 and PICT2017-0232), Consejo Nacional de
609 Investigaciones Cientificas y Técnicas (CONICET, PIP-0200), Comisión de
610 Investigaciones Cientificas (CIC-PBA) and Universidad Nacional de Mar del
611 Plata; a grant to GCP from the Howard Hughes Medical Institute (IECS award
612 55007430). LAA and JF are fellows of CONICET; NLA is a fellow of ANPCyT;
613 DFF, GCP, CAC and SD are researchers from CONICET.

Figure Legends

Figure 1. BNP codes for a DC1 domain containing protein. (A) Schematic view of a region of Arabidopsis chromosome 2 (from 18,323,538 to 18,321,537 bp - TAIR10) showing BNP genomic location and bnp-1 and bnp-2 insertion sites. (B) BNP amino acid sequence with boxed DC1 domains. (C) Phylogenic tree of 140 DC1 domain containing proteins in Arabidopsis. Bootstrap test results (1000 replicates) of the major nodes are indicated. IDs of sequences grouped in clusters I to VIII are listed. (D) Alignment of BNP with its closest Arabidopsis homologs and CaDC1 (AEI52549), TaCHP (ACU80555), NtDC1a (BAF80452) and NtDC1b (BAF80453). Phylogenic tree with bootstrap test results (1000 replicates) for the alignment of the complete 18 sequences is shown. Amino acid region represented for each sequence is indicated. DC1 domains are framed, signature residues and binding loop regions are indicated (C=Cys, H=His, — = loop). Higher intensity in grey scale denotes higher sequence similarity.

Figure 2. Pollen development and germination is impaired in *bnp-1* mutants. (A) Quantification of phenotypes observed in *BNP/BNP* and *bnp-1/BNP* plants in *qrt1/qrt1* background. (B-E) Nuclear configuration types revealed by DAPI (4',6-Diamidino-2-phenylindole) staining. Bars = 10 µm. (F) Quantification of pollen tube germination in tetrads from *BNP/BNP* and *bnp-1/BNP* plants in *qrt1/qrt1* background. (G-K) Pollen tube germination in tetrads. Bars = 20 µm

Figure 3. *BNP* is expressed in pollen and young sporophytic tissues. (A-D) Confocal images showing BNP-GFP through microgametogenesis. (E-H) Overlay between DIC and GFP fluorescence. (A and E) Microspore tetrad, (B and F) released microspore, (C and G) bicellular stage and (D and H) tricellular stage. (I) Image showing a projection along the z axis of all planes showing GFP fluorescence. (J) Overlay of DIC and GFP fluorescence showing a germinating pollen grain. (K-S) GUS activity in Arabidopsis transgenic plants carrying the *pBNP:GUS* construct. (K) Seedling 24 h after imbibition, (L) 48 h

after imbibition, (M) 6 days post germination and (N) 12 days post germination. (O) Root with lateral root primordium, (P) primary root with root hairs, (Q) third leaf 8 days after imbibition (R) third leaf 14 days after imbibition. (S) GUS signal was detected inside anthers at floral developmental stage 10. Three independent transgenic lines were used for this study. Pictures are representative of the results obtained in all analyzed lines. Bars = 10 µm.

Figure 4. BNP interacts with itself, VOZ1 and VOZ2. Bimolecular fluorescence complementation (BiFC) analysis of the interaction of BNP with itself, VOZ1 and VOZ2 in *Nicotiana benthamiana* leaves. Representative confocal microscopy images showing that BNP interacts with (A–C) itself, (D-F) VOZ1 and (G-I) VOZ2. Reconstituted YFP fluorescence (YFP) or DIC images of *N. benthamiana* leaves are shown in epidermal cells co-infiltrated with *Agrobacterium tumefaciens* harboring the indicated constructs. Control *N. benthamiana* leaves transfected with (J-L) BNP-N-YFP, (M-O) BNP-C-YFP, (P-R) VOZ1-C-YFP, (S-U) VOZ2-C-YFP do not show any BiFC signal. The last row (C, F, I, L, O, R, U) correspond to the magnification of regions of interest (insets) indicated in the first row. Bars = 20 µm.

Figure 5. BNP co-localizes with VOZ1 and VOZ2 to prevacuolar compartments. (A, F, K and P) Localization of BNP-GFP transiently expressed in *Nicotiana benthamiana* epidermal cells. (B) Fluorescent marker for prevacuolar compartments, RFP-Rha1. (C) Merged image of BNP-GFP and RFP-Rha1. (D) Shows an overlay with the corresponding bright-field image. (E, J, O and T) Pearson and Spearman correlation (PSC) test calculated using a plugin for ImageJ; r values indicate the level of co-localization ranging from +1 for perfect co-localization to −1 for negative correlation. (G) Fluorescent marker for Golgi apparatus, St-RFP. (H) Merged image of BNP-GFP and St-RFP. (I) Shows an overlay with the corresponding bright-field image. (L) Localization of RFP-VOZ1. (M) Merged image of BNP-GFP and RFP-VOZ1. (N) Shows the corresponding bright field image of the cells showed in (M). (Q) Localization of RFP-VOZ2. (R) Merged image of BNP-GFP and RFP-VOZ2. (S) Bright field image of the cells showed in (R). Bars = 20 µm.

679 **Figure 6. Nuclear localization of VOZ1 is affected in *bnp* mutants.**

680 Pollen tetrads from *qrt1/qrt1, BNP/BNP, VOZ1-RFP* (A, B, E, F, I, J) and
681 *qrt1/qrt1, bnp-1/BNP, VOZ1-RFP* (C, D, G, H, K, L) plants were analyzed at
682 microspore (A-D), binucleate (E-H) and mature tricellular (I-L) stages.
683 Representative z-stack images of confocal micrographs displaying VOZ1-RFP
684 fluorescence (B, D, F, H, J, L) and bright field images (A, C, E, G, I, K) are
685 shown. Arrowheads indicate nuclear localized VOZ1. Bars = 10 μm.
686 Mature pollen tetrads from four *qrt1/qrt1, BNP/BNP, VOZ1-RFP* and three
687 *qrt1/qrt1, bnp-1/BNP, VOZ1-RFP* plants were analyzed by fluorescent
688 microscopy and VOZ1 localization (M) and nuclear configuration (N) were
689 scored. Observed number and total pollen tetrads are indicated in parenthesis.
690

Table 1. Transmission efficiency of *bnp* alleles. Transmission efficiency of the *bnp-1* and *bnp-2* alleles in reciprocal crosses between mutant and WT plants.

Parental genotypes		Genotype of progeny† Number of individuals		Transmission efficiency of:	p-value*
Female	Male	WT	*bnp-1/BNP*	*bnp-1*	
bnp-1/BNP	WT	98	89	♀ 90.8%	0.51
WT	*bnp-1/BNP*	181	28	♂ 15.5%	<0.0001
		WT	*bnp-2/ BNP*	*bnp-2*	
bnp-2/BNP	WT	217	208	♀ 95.9%	0.66
WT	*bnp-2/BNP*	254	56	♂ 22%	<0.0001

†No homozygous plants were detected; * Chi-square test for a 1:1 segregation hypothesis (degrees of freedom = 1).

Table 2. Viability of the progeny in *bnp* mutants. Seed germination and seedling lethality of the progeny of self-pollinated *bnp-1/BNP*, *bnp-2/BNP* and WT plants.

Parental genotype	% viable progeny	% unviable progeny		p-value*
		not germinated	seedling lethality	
WT	98.86 (435/440)	0.23 (435/440)	1.13 (435/440)	
bnp-1/BNP	94.83 (715/754)	1.72 (13/754)	3.45 (26/754)	<0.001
bnp-2/BNP	93.32 (908/753)	2.15 (21/753)	4.52 (44/753)	<0.00001

In parenthesis, number of individuals observed over the total analyzed. * Chi-square test for a hypothesis of no relationship between the genotype of the parents and the viability of the progeny (degree of freedom = 1).

Parsed Citations

Alexander MP (1969) Differential Staining of Aborted and Nonaborted Pollen. Stain Technol 44: 117-122
Google Scholar: Author Only Title Only Author and Title

Alonso JM, Stepanova AN, Leisse TJ, Kim CJ, Chen H, Shinn P, Stevenson DK, Zimmerman J, Barajas P, Cheuk R, al e (2003) Genome-wide insertional mutagenesis of Arabidopsis thaliana. Science 301: 653–657
Google Scholar: Author Only Title Only Author and Title

Bhaskar RV, Mohanty B, Verma V, Wijaya E, Kumar PP (2015) A hormone-responsive C1-domain-containing protein At5g17960 mediates stress response in Arabidopsis thaliana. PLoS ONE 10: e0115418
Google Scholar: Author Only Title Only Author and Title

Boavida LC, McCormick S (2007) Temperature as a determinant factor for increased and reproducible in vitro pollen germination in Arabidopsis thaliana. Plant J 52: 570-582
Google Scholar: Author Only Title Only Author and Title

Bolte S, Talbot C, Boutte Y, Catrice O, Read ND, Satiat-Jeunemaitre B (2004) FM-dyes as experimental probes for dissecting vesicle trafficking in living plant cells. J Microsc 214: 159-173
Google Scholar: Author Only Title Only Author and Title

Borg M, Brownfield L, Twell D (2009) Male gametophyte development: A molecular perspective. J Exp Bot 60: 1465-1478
Google Scholar: Author Only Title Only Author and Title

Celesnik H, Ali GS, Robison FM, Reddy AS (2013) Arabidopsis thaliana VOZ (Vascular plant One-Zinc finger) transcription factors are required for proper regulation of flowering time. Biol Open 2: 424-431
Google Scholar: Author Only Title Only Author and Title

Clough SJ, Bent AF (1998) Floral dip: a simplified method for Agrobacterium-mediated transformation of Arabidopsis thaliana. Plant J 16: 735-743
Google Scholar: Author Only Title Only Author and Title

Colon-Gonzalez F, Kazanietz MG (2006) C1 domains exposed: from diacylglycerol binding to protein-protein interactions. Biochim Biophys Acta 1761: 827-837
Google Scholar: Author Only Title Only Author and Title

Curtis MD, Grossniklaus U (2003) A gateway cloning vector set for high-throughput functional analysis of genes in planta. Plant Physiol 133: 462–469.
Google Scholar: Author Only Title Only Author and Title

D'Ippólito S, Arias LA, Casalongué CA, Pagnussat GC, Fiol DF (2017) The DC1-domain protein VACUOLELESS GAMETOPHYTES is essential for female and male gametophyte development in Arabidopsis. Plant J 90: 261-275
Google Scholar: Author Only Title Only Author and Title

Escobar-Sepúlveda HF, Trejo-Téllez LI, Pérez-Rodríguez P, Hidalgo-Contreras JV, Gómez-Merino FC (2017) Diacylglycerol kinases are widespread in higher plants and display inducible gene expression in response to beneficial elements, metal, and metalloid ions. Front Plant Sci 8: 129
Google Scholar: Author Only Title Only Author and Title

Foresti O, Gershlick DC, Bottanelli F, Hummel E, Hawes C, Denecke J (2010) A recycling-defective vacuolar sorting receptor reveals an intermediate compartment situated between prevacuoles and vacuoles in tobacco. Plant Cell 22: 3992-4008
Google Scholar: Author Only Title Only Author and Title

Formstecher E, Aresta S, Collura V, Hamburger A, Meil A, Trehin A, Reverdy C, Betin V, Maire S, Brun C, Jacq B, Arpin M, Bellaiche Y, Bellusci S, Benaroch P, Bornens M, Chanet R, Chavrier P, Delattre O, Doye V, Fehon R, Faye G, Galli T, Girault JA, Goud B, de Gunzburg J, Johannes L, Junier MP, Mirouse V, Mukherjee A, Papadopoulo D, Perez F, Plessis A, Rosse C, Saule S, Stoppa-Lyonnet D, Vincent A, White M, Legrain P, Wojcik J, Camonis J, Daviet L (2005) Protein interaction mapping: a Drosophila case study. Genome Res 15: 376-384
Google Scholar: Author Only Title Only Author and Title

Francis KE, Lam SY, Copenhaver GP (2006) Separation of Arabidopsis pollen tetrads is regulated by QUARTET1, a pectin methylesterase gene. Plant Physiol 142: 1004-1013
Google Scholar: Author Only Title Only Author and Title

French AP, Mills S, Swarup R, Bennett MJ, Pridmore TP (2008) Colocalization of fluorescent markers in confocal microscope images of plant cells. Nat Protoc 3: 619-628
Google Scholar: Author Only Title Only Author and Title

Fromont-Racine M, Rain JC, Legrain P (1997) Toward a functional analysis of the yeast genome through exhaustive two-hybrid screens. Nat Genet 16: 277-282

Google Scholar: Author Only Title Only Author and Title

Gao S, Yang L, Zeng HQ, Zhou ZS, Yang ZM, Li H, Sun D, Xie F, Zhang B (2016) A cotton miRNA is involved in regulation of plant response to salt stress. Sci Reports 6: 19736

Google Scholar: Author Only Title Only Author and Title

Grefen C, Donald N, Hashimoto K, Kudla J, Schumacher K, Blatt MR (2010) A ubiquitin-10 promoter-based vector set for fluorescent protein tagging facilitates temporal stability and native protein distribution in transient and stable expression studies. Plant J 64: 355-365

Google Scholar: Author Only Title Only Author and Title

Hafidh S, Fila J, Honys D (2016) Male gametophyte development and function in angiosperms: a general concept. Plant Reprod 29: 31-51

Google Scholar: Author Only Title Only Author and Title

Heslop-Harrison J, Heslop-Harrison Y (1970) Evaluation of pollen viability by enzymatically induced fluorescence; intracellular hydrolysis of fluorescein diacetate. Stain Technol 45: 115-120

Google Scholar: Author Only Title Only Author and Title

Hwang IS, Choi DS, Kim NH, Kim DS, Hwang BK (2014) The pepper cysteine/histidine-rich DC1 domain protein CaDC1 binds both RNA and DNA and is required for plant cell death and defense response. New Phytol 201: 518-530

Google Scholar: Author Only Title Only Author and Title

Jensen Michael K, Kjaersgaard T, Nielsen Michael M, Galberg P, Petersen K, O'Shea C, Skriver K (2010) The Arabidopsis thaliana NAC transcription factor family: structure–function relationships and determinants of ANAC019 stress signalling. Biochem J 426: 183-196

Google Scholar: Author Only Title Only Author and Title

Johnson-Brousseau SA, McCormick S (2004) A compendium of methods useful for characterizing Arabidopsis pollen mutants and gametophytically-expressed genes. Plant J 39: 761-775

Google Scholar: Author Only Title Only Author and Title

Kearse M, Moir R, Wilson A, Stones-Havas S, Cheung M, Sturrock S, Buxton S, Cooper A, Markowitz S, Duran C, Thierer T, Ashton B, Meintjes P, Drummond A (2012) Geneious Basic: an integrated and extendable desktop software platform for the organization and analysis of sequence data. Bioinformatics 28: 1647-1649

Google Scholar: Author Only Title Only Author and Title

Koguchi M, Yamasaki K, Hirano T, Sato MH (2017) Vascular plant one-zinc-finger protein 2 is localized both to the nucleus and stress granules under heat stress in Arabidopsis. Plant Signal Behav 12: e1295907

Google Scholar: Author Only Title Only Author and Title

Kumar S, Choudhary P, Gupta M, Nath U (2018) VASCULAR PLANT ONE-ZINC FINGER1 (VOZ1) and VOZ2 Interact with CONSTANS and promote photoperiodic flowering transition. Plant Physiol 176: 2917-2930

Google Scholar: Author Only Title Only Author and Title

Kumar S, Stecher G, Tamura K (2016) MEGA7: molecular evolutionary genetics analysis version 7.0 for bigger datasets. Mol Biol Evol 33: 1870-1874

Google Scholar: Author Only Title Only Author and Title

Lalanne E, Twell D (2002) Genetic control of male germ unit organization in Arabidopsis. Plant Physiol 129: 865-875

Google Scholar: Author Only Title Only Author and Title

León G, Holuigue L, Jordana X (2007) Mitochondrial Complex II is essential for gametophyte development in Arabidopsis. Plant Physiol 143: 1534-1546

Google Scholar: Author Only Title Only Author and Title

Li C, Lv J, Zhao X, Ai X, Zhu X, Wang M, Zhao S, Xia G (2010) TaCHP: A wheat zinc finger protein gene down-regulated by abscisic acid and salinity stress plays a positive role in stress tolerance. Plant Physiol 154: 211-221

Google Scholar: Author Only Title Only Author and Title

Mimida N, Kidou S, Iwanami H, Moriya S, Abe K, Voogd C, Varkonyi-Gasic E, Kotoda N (2011) Apple FLOWERING LOCUS T proteins interact with transcription factors implicated in cell growth and organ development. Tree Physiol 31: 555-566

Google Scholar: Author Only Title Only Author and Title

Mitsuda N, Hisabori T, Takeyasu K, Sato MH (2004) VOZ; isolation and characterization of novel vascular plant transcription factors with a one-zinc finger from Arabidopsis thaliana. Plant Cell Physiol 45: 845-854

Google Scholar: Author Only Title Only Author and Title

Nakai Y, Nakahira Y, Sumida H, Takebayashi K, Nagasawa Y, Yamasaki K, Akiyama M, Ohme-Takagi M, Fujiwara S, Shiina T, Mitsuda N, Fukusaki E, Kubo Y, Sato MH (2013) Vascular plant one-zinc-finger protein 1/2 transcription factors regulate abiotic and biotic stress responses in Arabidopsis. Plant J 73: 761-775

Google Scholar: Author Only Title Only Author and Title

Pagnussat GC, Yu HJ, Ngo QA, Rajani S, Mayalagu S, Johnson CS, Capron A, Xie LF, Ye D, Sundaresan V (2005) Genetic and molecular identification of genes required for female gametophyte development and function in Arabidopsis. Development 132: 603-614

Google Scholar: Author Only Title Only Author and Title

Pagnussat GC, Yu HJ, Sundaresan V (2007) Cell-fate switch of synergid to egg cell in Arabidopsis eostre mutant embryo sacs arises from misexpression of the BEL1-like homeodomain gene BLH1. Plant Cell 19: 3578-3592

Google Scholar: Author Only Title Only Author and Title

Palfy M, Remenyi A, Korcsmaros T (2012) Endosomal crosstalk: meeting points for signaling pathways. Trends Cell Biol 22: 447-456

Google Scholar: Author Only Title Only Author and Title

Pyrzynska B, Pilecka I, Miaczynska M (2009) Endocytic proteins in the regulation of nuclear signaling, transcription and tumorigenesis. Mol Oncol 3: 321-338

Google Scholar: Author Only Title Only Author and Title

Rahman GM, Das J (2015) Modeling studies on the structural determinants for the DAG/phorbol ester binding to C1 domain. J Biomol Struct Dyn 33: 219-232

Google Scholar: Author Only Title Only Author and Title

Schwarzenbacher RE, Wardell G, Stassen J, Guest E, Zhang P, Luna E, Ton J (2020) The IBI1 receptor of β-aminobutyric acid interacts with VOZ transcription factors to regulate abscisic acid signaling and callose-associated defense. Molecular Plant 13: 1455-1469

Google Scholar: Author Only Title Only Author and Title

Selote D, Matthiadis A, Gillikin JW, Sato MH, Long TA (2018) The E3 ligase BRUTUS facilitates degradation of VOZ1/2 transcription factors. Plant Cell Environ 41: 2463-2474

Google Scholar: Author Only Title Only Author and Title

Serrano I, Buscaill P, Audran C, Pouzet C, Jauneau A, Rivas S (2016) A non canonical subtilase attenuates the transcriptional activation of defence responses in Arabidopsis thaliana. Elife 5

Google Scholar: Author Only Title Only Author and Title

Shinya T, Galis I, Narisawa T, Sasaki M, Fukuda H, Matsuoka H, Saito M, Matsuoka K (2007) Comprehensive analysis of glucan elicitor-regulated gene expression in tobacco BY-2 cells reveals a novel MYB transcription factor involved in the regulation of phenylpropanoid metabolism. Plant Cell Physiol 48: 1404-1413

Google Scholar: Author Only Title Only Author and Title

Song C, Lee J, Kim T, Hong JC, Lim CO (2018) VOZ1, a transcriptional repressor of DREB2C, mediates heat stress responses in Arabidopsis. Planta 247: 1439-1448

Google Scholar: Author Only Title Only Author and Title

Suesslin C, Frohnmeyer H (2003) An Arabidopsis mutant defective in UV-B light-mediated responses. Plant J 33: 591-601

Google Scholar: Author Only Title Only Author and Title

Twell D (2011) Male gametogenesis and germline specification in flowering plants. Sex Plant Reprod 24: 149-160

Google Scholar: Author Only Title Only Author and Title

Wang J, Wang R, Fang H, Zhang C, Zhang F, Hao Z, You X, Shi X, Park CH, Hua K, He F, Bellizzi M, Xuan Vo KT, Jeon J-S, Ning Y, Wang G-L (2021) Two VOZ transcription factors link an E3 ligase and an NLR immune receptor to modulate immunity in rice. Molecular Plant 14: 253-266

Google Scholar: Author Only Title Only Author and Title

Wee EG-T, Sherrier DJ, Prime TA, Dupree P (1998) Targeting of active sialyltransferase to the plant golgi apparatus. Plant Cell 10: 1759-1768

Google Scholar: Author Only Title Only Author and Title

Wu P, Wee P, Jiang J, Chen X, Wang Z (2012) Differential regulation of transcription factors by location-specific EGF receptor signaling via a spatio-temporal interplay of ERK activation. PLoS One 7: e41354

Google Scholar: Author Only Title Only Author and Title

Yasui Y, Kohchi T (2014) VASCULAR PLANT ONE-ZINC FINGER1 and VOZ2 repress the FLOWERING LOCUS C clade members to control flowering time in Arabidopsis. Biosci Biotechnol Biochem 78: 1850-1855

Google Scholar: Author Only Title Only Author and Title

Yasui Y, Mukougawa K, Uemoto M, Yokofuji A, Suzuri R, Nishitani A, Kohchi T (2012) The phytochrome-interacting vascular plant one-zinc finger1 and VOZ2 redundantly regulate flowering in Arabidopsis. Plant Cell 24: 3248-3263

Google Scholar: Author Only Title Only Author and Title

Zuckerkandl E, Pauling L (1965) Evolutionary divergence and convergence in proteins. Evolving genes and proteins 97: 97-166